



Low Cycle Mechanical and Fatigue Properties of AlZnMgCu Alloy

S. Pysz^{a*}, E. Czekaj^a, R. Żuczek^a, M. Maj^b, J. Piekło^b

^a Foundry Research Institute, 73 Zakopianska Str., 30-418 Cracow, Poland

^b AGH University of Science and Technology, Faculty of Foundry Engineering, Department of Foundry Process Engineering, 23 Reymonta Str., 30-059 Cracow, Poland

* Corresponding author. E-mail address: stanislaw.pysz@iod.krakow.pl

Received 16.06.2015; accepted in revised form 17.07.2015

Abstract

The article presents the analysis of properties of the high-strength AlZnMgCu (abbr AlZn) aluminium alloy and estimates possibilities of its application for responsible structures with reduced weight as an alternative to iron alloy castings. The aim of the conducted studies was to develop and select the best heat treatment regime for a 7xx casting alloy based on high-strength materials for plastic working from the 7xxx series. For analysis, wrought AlZnMgCu alloy (7075) was selected. Its potential of the estimated as-cast mechanical properties indicates a broad spectrum of possible applications for automotive parts and in the armaments industry. The resulting tensile and fatigue properties support the thesis adopted, while the design works further confirm these assumptions.

Keywords: High-strength aluminium alloy, Low-cycle fatigue test, Mechanical properties

1. Introduction

The ecological aspect of structural elements optimization in terms of material change and weight reduction is of a primary importance in the automotive industry, the more that efforts to increase the comfort of use are unavoidably associated with increased total weight of the vehicle. The necessity to meet the latest emission standards for harmful compounds of the combustion process forces manufacturers to look for new solutions. Depending on the intended conditions of use, the design of structures with the reduced weight is here particularly advantageous, since the estimated vehicle weight reduction of about 100 kg means saving of up to 0.5 litres of fuel per every 100 km [1, 2]. The tendency to reduce the vehicle weight is clearly seen on the example of Audi, where most of the steel elements were replaced with aluminium structures in Audi A8, and in the TT sports cars, the skeleton frame and fragments of body panelling were designed as a hybrid combination of steel

and aluminium elements reducing the weight of the frame by 48% [3]. In the case of special purpose vehicles, including the vehicles for military applications, weight reduction is often a secondary factor. Mobility of the vehicle or possibility of air transport is often at odds with increased resistance to the risk of explosion obtained through the use of protective armour. In this case, however, the priority is to ensure the protection of conveyed passengers and transported equipment, and provide full mobility in case of minor damages caused by the ravaging effect of improvised explosive devices (IED) [4 - 6]. The materials most commonly used nowadays include, continuously improved, steels of common and special types, whose specific weight is approximately 7800 kg/m³. Growing popularity also enjoy the composite materials, combining high strength with good damping properties and low specific weight. A disadvantage of such solutions is the high manufacturing cost of composite structures compared to steel or aluminium alloys (Fig. 1).

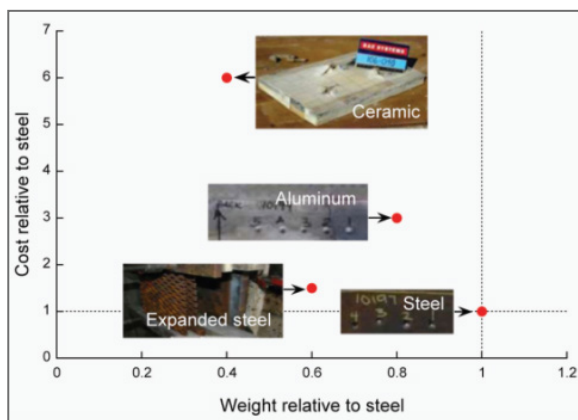


Fig. 1. The cost per unit weight of parts for selected groups of materials used in the armaments industry [7]

More and more frequently is discussed the possibility to use aluminium alloys in special purpose vehicles, because of the three times lower specific weight. The use of high strength aluminium alloys can significantly reduce the weight of the structure, while offering similar, or sometimes even higher, strength properties compared to materials based on iron. This is not possible in all aspects of the changes carried out, but profiled aluminium structures are capable of carrying similar loads as structures made of iron alloys used so far.

Aluminium alloys are most widely used in the aerospace industry where weight reduction is critical for an aircraft. In air

transport, the most commonly used aluminium alloys are Al-Mg alloys from the 2xxx group, mainly alloys designated by the symbols 2014 and 2024 with subsequent modifications. The second group consists of high-strength 7xxx series wrought alloys, for which the tensile strength after appropriate treatment reaches more than 600 MPa. These alloys are commonly used in aircraft constructions for, among others, frames, beams, ribs of aircraft wings, or panelling elements [8].

Depending on the application or loads to be carried, the use of aluminium castings, as a replacement for parts made of iron alloys, reducing the unit weight of the structure by 10 to 50%.

Lightweight components, manufactured from aluminium alloys, in addition to weight reduction, are also capable of offering a number of other advantages to the designers. They are characterized by high levels of functionality (material indices) such as unit stiffness parameters (e.g. E/ρ) and mechanical strength (e.g. $R_{p0.2}/\rho$), presented in Table 1, or optionally fracture toughness (K_{Ic}/ρ).

The components made of aluminium alloys are also expected to have good resistance to thermal and mechanical fatigue, good dimensional stability, minimum porosity in the case of cast structures, resistance to chemical and electro-chemical corrosion, etc. Examples of data in Table 1 show that aluminium and its alloys are characterized by very high unit indicators of functionality compared with heavy metals (and their alloys) based on Fe, Cu or Zn.

Table 1. Some functionality indicators (material indices) of selected casting alloys. [9 - 10]

Alloy	Density ρ , [Mg/m ³]	Young's modulus E , [GPa]	Yield strength, $R_{p0.2}$, [MPa]	Functionality indicators (material indices)					
				M_1	M_2	M_3	M_4	M_5	M_6
				E/ρ	$E^{1/2}/\rho$	$E^{1/3}/\rho$	$(R_{p0.2})/\rho$	$(R_{p0.2})^{1/2}/\rho$	$(R_{p0.2})^{2/3}/\rho$
aluminium	2.70	70	300	25.93	3.10	1.53	111.11	6.42	16.60
iron	7.85	200	1100	25.48	1.80	0.74	140.13	4.22	13.57
copper	8.93	124	500	13.89	1.25	0.56	55.99	2.50	7.05
zinc	7.13	84	250	11.78	1.29	0.61	35.06	2,22	5.57

Note! The values of the density ρ and Young's modulus E refer to technically pure elements given very insignificant differences observed in alloys based on these elements; the values of the yield strength $R_{p0.2}$ are average values obtained for a given group of alloys.

2. Alloy preparation and making specimens for mechanical tests

Studies were undertaken to examine the possibility of using alloy 7075 as a material for cast structures. Although this alloy is not a conventional casting alloy and its high mechanical properties are obtained in the wrought condition, it has a great potential applicability for high strength cast structural parts operating in various constructions, mainly due to the combination of chemical composition involving zinc, magnesium and copper. The high strength of AlZnMgCu alloys, widely used in aviation for structural components made as forgings or parts machined

after plastic forming, encourages the use of casting technology, which allows obtaining structures with similar functional properties. The specific thermo-physical properties of the AlZnMgCu alloy characterized by, among others, a wide degree of solidification temperatures are the reason why making castings for high performance applications should go hand in hand with the development of a suitable composition, heat treatment regime and casting technology, and only proper combination of all these factors can guarantee successful manufacture of cast AlZnMgCu alloy components with structure that will provide strength in excess of 450 MPa at an elongation of about 3%. A large part of the literature describing studies and determination of the properties of selected AlZn alloys refers to wrought alloys, the

use of which for castings is still at the stage of preliminary research.

The strength of AlZnMgCu alloys generally increases with the increasing content of Zn and Mg, but an adverse consequence is higher susceptibility to hot cracking during casting and rapid cooling, especially for the Zn content of more than 7%. An equally important problem is the very low or even nil ductility in castings used as finished structural elements, mainly due to the process of phase transformations taking place during solidification, and the risk of high porosity resulting, among others, from a wide range of the solidification temperatures. Interesting and contributing a lot to better understanding of the process of microstructure formation during solidification of 7XXX alloys are studies described, among others, in [11 - 13].

For the tests and studies described in this article, an alloy containing (composition in wt.%): Zn - 5.53; Mg - 2.37; Cu - 4.56; Fe - 0.2; Si - 0.1 was selected.

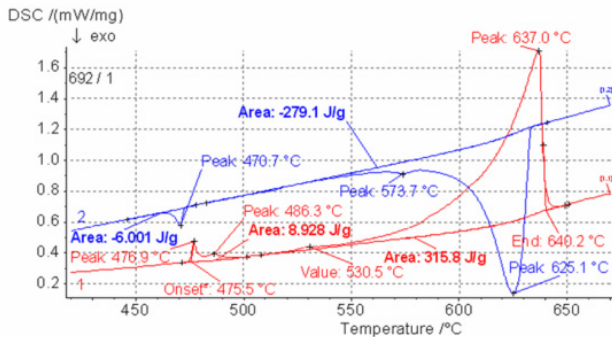


Fig. 2. Experimental DSC curve plotted for selected alloy

Based on the analysis of DSC curves (Fig. 2) and literature data, for the test alloy, the following parameters of multi-stage heat treatment were selected:

- solution heat treatment: 450°C (4 h) + 470°C (4 h);
- aging: 110°C (5 h) + 160°C (10 h).

Preliminary mechanical tests based on the static tensile test have revealed that for the proposed chemical composition and heat treatment parameters, the strength obtained on samples gravity poured in a die amounted to an average of about 430 MPa, but the obtained values of elongation did not exceed 1%. So, further research focussed on a modification of the heat treatment process to increase the examined values to the desired level.

Optimization of the heat treatment parameters was carried out on the casting of control arm made from an aluminium alloy. The test castings were made in ceramic moulds without cooling and with cooling by immersion in a specially prepared cooling medium. Testing of basic mechanical properties was performed on flat samples cut out from selected places on the cast control arm shown in Fig. 3. Standard samples subjected to the same heat treatment were also used.

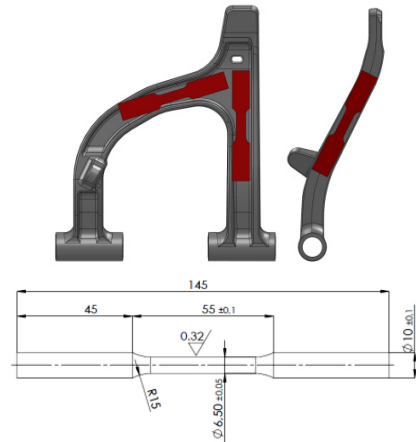


Fig. 3. Model of control arm - note marking of places where samples were taken for testing; the drawing below shows the shape and dimensions of the specimen used in testing of mechanical properties

Basing on the analysis of source materials, own experience of the authors and executors of a project implemented in the Foundry Research Institute, and using the results of preliminary tests, optimal parameters of the heat treatment to the T6 condition were finally established for components cast from the AlZnMgCu alloy. The choice was multi-stage solutioning and aging carried out under the following conditions:

I – solutioning (multi-stage): 0.5h to 450°C, 2h at 450°C, 0.5h to 530°C, 2h at 530°C, 0.25h to 560°C, 2h at 560°C – cooling in water at 80°C;

II - aging (different variants): 0.5h to 120°C, 4h at 120°C, 0.5h to 150°C, 8h at 150°C – cooling with furnace

3. Low cycle tensile and fatigue testing

The aim of the studies was to determine the mechanical properties, fatigue behaviour included, of high strength AlZnMgCu aluminium alloy based on data obtained from the low cycle tensile and fatigue tests. To determine the mechanical properties of the alloy, a modified low cycle fatigue test (MLCF) was applied as a tool for the specification of parameters resulting from the Manson-Coffin-Morrow relationship [14]:

$$\epsilon_{max} = \frac{1}{2}\Delta\epsilon_c = \frac{1}{2}\Delta\epsilon_{as} + \frac{1}{2}\Delta\epsilon_{apl} = \frac{\sigma_f}{E}(2N_f)^b + \epsilon_f'(2N_f)^c \quad (1)$$

where:

$\Delta\epsilon_c$ – the total strain amplitude,

$\Delta\epsilon_{as}$ – the elastic strain amplitude,

$\Delta\epsilon_{apl}$ – the plastic strain amplitude,

σ_f – the fatigue life coefficient approximately equal to the tensile strength R_m ,

ϵ_f' – the true permanent strain induced by stress σ_f ,

$2N_f$ – the number of load cycles to specimen failure,

ϵ_p – the true permanent strain induced by $2N_f$ load cycles,

b – fatigue strength exponent,

c – fatigue ductility exponent.

The fatigue strength Z_{go} , necessary for calculation of the MLCF test parameters is assessed from the experimental graph (Fig. 4) plotted for a diverse group of materials, starting with pure metals and ending in alloys of the ferrous and non-ferrous metals [15].

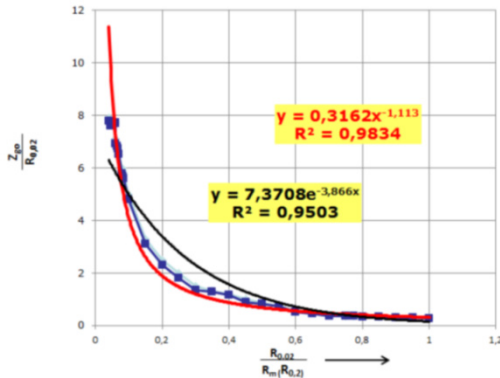


Fig. 4. Curve for the evaluation of fatigue strength [15]

To determine the values of b , c , and ε_{max} , the following assumptions were adopted [16, 17]:

- disorders in uniaxial compressive stress field are eliminated by the use of one-sided load cycles (during tension) in a fatigue test,
- the permanent strain induced by a preset small number of cycles (e.g. twenty load-unload cycles) shows a dependence on the cycle amplitude similar to the strain suffered by the sample on failure, the more that its value after 20 cycles changes only slightly under the higher number of cycles or does not change at all,
- the mechanical properties mentioned above are calculated on one sample only, which is a major advantage of the MLCF fatigue test,
- the course of the straight lines from equations (2) and (3) in double logarithmic scale is determined from the position of points with coordinates $(\ln 20, \ln R_m)$ and $(\ln 2N_f, \ln Z_{go})$ for equation (2) and $(\ln 20, \ln \varepsilon_f)$ and $(\ln 2N_f, \ln \varepsilon_z)$ for equation (3).

$$\sigma_a = \sigma_f (2N_f)^b \quad (2)$$

$$\varepsilon_p = \varepsilon_f (2N_f)^c \quad (3)$$

where:

σ_a – the stress cycle amplitude,

ε_p – the true permanent strain induced by $2N_f$ load cycles at $\varepsilon_p = \ln(1 + \varepsilon_k)$, $\varepsilon_k = \Delta l_{trwale} / l_0$,

ε_z – the true permanent strain corresponding to the fatigue life limit.

MLCF tests were performed on 6.5 mm diameter samples in a positive pulsating cycle with increasing stress amplitude. On samples of selected materials, static tensile test was also carried out to assess the tensile strength of AlZnMgCu alloy [18, 19]. The stress-strain curves obtained for selected samples are plotted in Fig. 5 - 7 as a function of the adopted cooling rate.

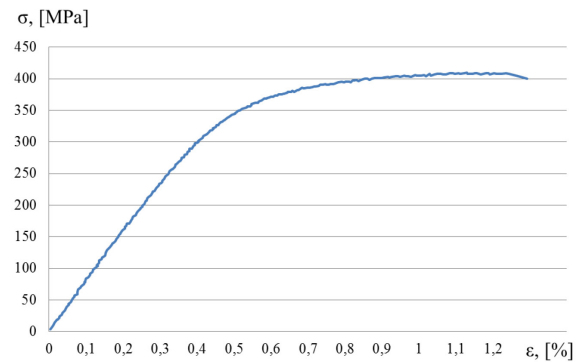


Fig. 5. The stress-strain curve ($\sigma - \varepsilon$) obtained in static tensile test for the sample of AlZn_T6_1R alloy

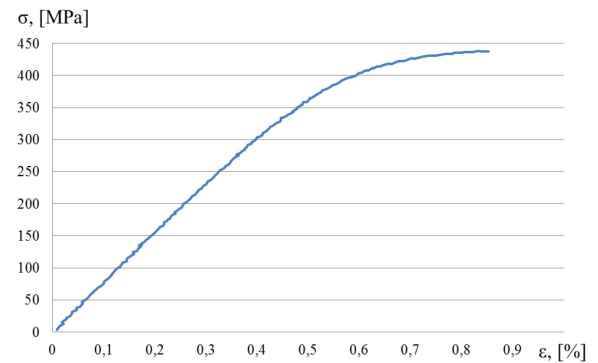


Fig. 6. The stress-strain curve ($\sigma - \varepsilon$) obtained in static tensile test for the sample of 10AlZn_T6_3B alloy

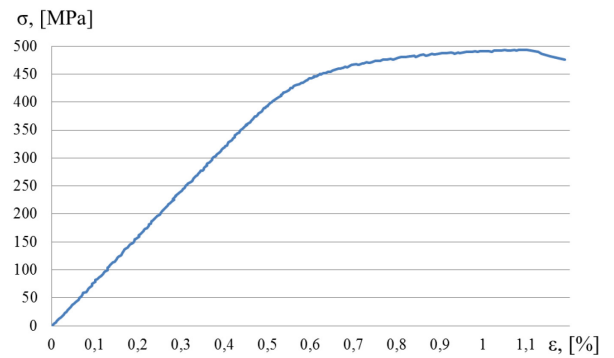


Fig. 7. The stress-strain curve ($\sigma - \varepsilon$) obtained in static tensile test for the sample of 5AlZn_T6_3A alloy

The results of preliminary mechanical tests were used in further fatigue tests during which the following parameters were determined: the tensile strength R_m , elongation A , the yield strength $R_{0,2}$, the apparent elastic limit $R_{0,02}$, and the apparent limits $R_{0,1}$ and $R_{0,05}$ for 0.1 % and 0.05% permanent strain, the modulus of elasticity E_{80} and E_{180} , under a load corresponding to 80 MPa and 180 MPa, respectively, the rotary bending fatigue strength Z_{go} , the maximum acceptable total permanent strain ε_{max} ,

in this case for the number of $100 \cdot 10^6$ cycles, the fatigue strength exponent b and the fatigue ductility exponent c . Calculations were based on respective values of force displacements read out from the charts listed below (Figs. 8 and 9) showing the stress-strain (elongation) relationships obtained from the MLCF fatigue tests, based on which the above mentioned mechanical properties were determined.

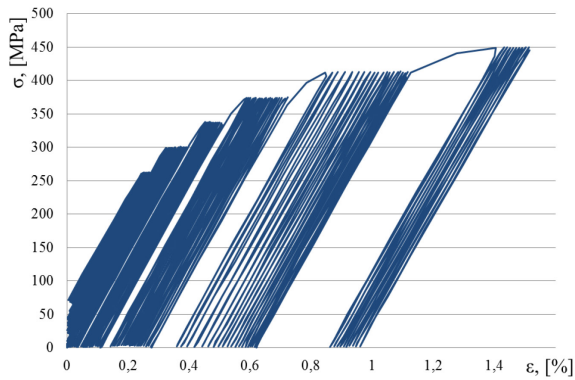


Fig. 8. The stress-strain curve ($\sigma - \epsilon$) obtained for the sample of 10AlZn_T6_3B_M1 alloy

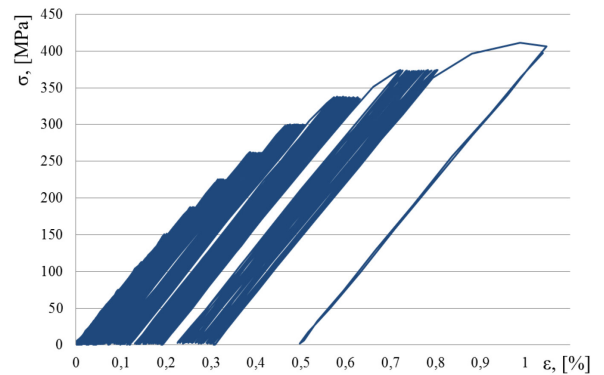


Fig. 9. The stress-strain curve ($\sigma - \epsilon$) obtained for the sample of 5AlZn_T6_3A_M2 alloy

The values of the coefficients b and c determined by the MLCF test are presented in Table 2, while the results of calculations based on fatigue tests (rows 1ZM, M1, M2) in accordance with the MLCF algorithm and the results of static tensile tests (row R) are summarized in Table 3.

Table 2.

The coefficients b and c in the Manson-Coffin-Morrow relationship calculated for selected samples

	10AlZn_T6_3B_M1	5AlZn_T6_3A_M2
b	-0.08	-0.09
c	-0.18	-0.14

Table 3.

Mechanical properties of selected materials for various ranges of the cooling rates

	R_m [MPa]	A [%]	E_{80} [MPa]	E_{180} [MPa]	$R_{0,02}$ [MPa]	$R_{0,05}$ [MPa]	$R_{0,1}$ [MPa]	$R_{0,2}$ [MPa]	Z_{go} [MPa]	ϵ_{max} [%]
AlZn_T6										
R	407	1.2	81020	-	-	-	-	385	-	-
1ZM	448	1.1	82370	81546	360	387	412	421	199	0,410
10AlZn_T6_3B										
R	437	0.8	76200	-	-	-	-	435	-	-
M1	449	2.0	79500	79000	295	299	337	373	165	0.280
5AlZn_T6_3A										
R	492	1.1	77800	-	-	-	-	476	-	-
M2	411	1.0	70600	75705	182	225	300	351	121	0.240

4. Conclusions

The problem of the fatigue life estimation of a structure is connected, on the one hand, with the experimental determination of material characteristics while, on the other hand, it requires knowledge of the components of the state of stress and strain in the examined element. Fatigue tests are usually carried out under uniaxial load, and hence comes the problem of their effective application in the analysis of design robustness, which is generally subjected to the effect of multiaxial loads. The criteria

of multiaxial fatigue reduce the multi-axial state to a uniaxial one, which is used by standard tests for the fatigue life determination. The reduction is done with a relationship that links the components of the state of stress and strain; the criterion can also base on the determined energy of deformation. Among different criteria of the multiaxial fatigue, one can distinguish those that have been formulated basing on the concept of the, so-called, critical plane, which assumes that a fatigue crack is caused by the action of stress or strain which occur in this plane. The concept of critical plane specifies the location of the crack initiation, and as

such was initially used in the high-cycle fatigue test (HCF), although – as proved by numerous tests - it behaves quite well also in the range of the low number of fatigue cycles (LCF). The determination of the stress and strain components in the examined structure is generally carried out with programs using numerical methods such as FEM, where the description of the tested material is usually based on linear characteristics or on the stress-strain relationship above the yield point level. The estimation of fatigue life is done by comparing the state of strain in selected finite elements of the representative area of the structure with the fatigue life curve obtained for the alloy through the determination of coefficients b and c (Table 2), and through the determination of the allowable permanent strain ε_{\max} (Table 3). The state of strain in the components is subjected to analysis and is reduced to the equivalent deformation according to one of the hypotheses, or in the case of one dominant component may be identical with this component. The results obtained in this study can be used in an analysis of the fatigue life of structures cast from the examined aluminium alloys.

References

- [1] Koeth, C.P. (2007). Leichtbau - die Zweite, *Automobilindustrie* 3.
- [2] Feldmann, J. (2008). *Kunststoffe – Werkstoffe der Energieeffizienz; Kunststoffe im Automobilbau*, VDI - Verlag.
- [3] Idzior, M. (2009). Directions material changes in the automotive industry in light of the requirements of ecology. *MOTROL*, 9, 72-87. (in Polish).
- [4] Żuczek, R., Pysz, S. & Karwiński, A. (2009). Conversion of material and design element forged to castings. *Transactions of Foundry Research Institute*. 49(3), 23–36. Kraków.
- [5] Pysz, S. & Żuczek, R. (2012). The Use of ICME Process to Design a Rocker Arm for Special Purpose Vehicles. *TEKA Comission of Motorization and Energetics in Agroclulture*. 12(1), 205–210.
- [6] Żuczek, R., Pysz, S., Sprawka, P. & Muszyński, T. (2015). The innovative design of suspension cast components of vehicles made from high-strength AlZnMgCu alloy resistant to an IED type threat. *Solid State Phenomena*, (223), 181-190.
- [7] Application of Lightweighting Technology to Military Vehicles, Vessels, and Aircraft. Committee on Benchmarking the Technology and Application of Lightweighting, ISBN 978-0-309-22166-5, 2012.
- [8] Dymek, S. (2012). *Modern aluminium alloys wrought*. Kraków. Wydawnictwa AGH. (in Polish).
- [9] Ashby, M.F. (1998). *Materials Selection in Mechanical Design*. Warszawa. WNT.
- [10] *Use of Lightweight Materials in 21st Century Army Trucks*, Committee on Lightweight Materials for 21st Century Army Trucks, National Research Council, 2003 (<http://www.nap.edu/catalog/10662.html>, online: 01.2015).
- [11] Zyska, A., Konopka, Z., Łągiewka, M., Bober, A. & Nocuń, S. (2006). Modification of AlZn5Mg alloy. *Archive of Foundry* 6(22), 582-589.
- [12] Weiss, V., Svobodova, J. & Cais, J. (2014). The Crystal Segregation During Casting of the Alloy AlZn5.5Mg2.5Cu1.5. *Archives of Foundry Engineering* 14(2), 63-68.
- [13] Chinella, J.F., Guo, Z. (2011). *Computational Thermodynamics Characterization of 7075, 7039, and 7020 Aluminium Alloys Using JMatPro*. Army Research Laboratory Aberdeen Proving Ground, MD 21005-5069.
- [14] Kocańda, S., Szala, J. (1985). *Basis of calculation of fatigue*. Warszawa. PWN. (in Polish).
- [15] Maj, M. (2012). Fatigue life selected alloys. *Archives of Foundry Engineering*. Katowice - Gliwice. (in Polish).
- [16] Piekło, J. & Maj, M. (2014). Evaluation of casting fatigue life based on numerical model and fatigue tests. *Archives of Foundry Engineering*, 14(4), 95–100.
- [17] Maj, M., Pietrzak, K. & Piekło, J. (2013). Modified low cycle method as a new criterion for a life fatigue assessment in foundry industry. *Archives of Metallurgy and Materials*. 58(3), 877–881.
- [18] Maj, M., Pysz, S., Piekło, J. & Gazda, A. (2012). Fatigue testing of AlZnMgCu alloy used for parts of suspension system. *Inżynieria Materiałowa*. 33(6), 635-638.
- [19] Maj, M., Piekło, J. (2009). MLCF – An optimised program of low-cycle fatigue test to determine mechanical properties of cast materials. *Archives of Metallurgy and Materials vol. 54 iss. 2*. 393–397. Polish Academy of Sciences. Committee of Metallurgy. Institute of Metallurgy and Materials Science; ISSN 1733-3490.